
Proceedings Paper:
Lio, W.H., Jones, B.L. and Rossiter, J.A. orcid.org/0000-0002-1336-0633 (2017) Analysis and design of tower motion estimator for wind turbines. In: 2016 IEEE International Conference on Renewable Energy Research and Applications (ICRERA). ICRERA 2016, 20-23 November, 2016, Birmingham, UK. IEEE . ISBN 978-1-5090-3388-1

https://doi.org/10.1109/ICRERA.2016.7884416

Analysis and design of tower motion estimator for wind turbines

W. H. Lio*, B. Ll. Jones† and J. A. Rossiter‡
Department of Automatic Control and Systems Engineering, The University of Sheffield, Sheffield, S1 3JD, U.K.
E-mail: *w.h.lio@sheffield.ac.uk, †b.l.jones@sheffield.ac.uk, ‡j.a.rossiter@sheffield.ac.uk

***Abstract*—The use of blade individual pitch control (IPC) provides a means of alleviating the harmful turbine loads that arise from the uneven and unsteady forcing from the oncoming wind. Such IPC algorithms, which mainly target the blade loads at specific frequencies, are designed to avoid excitations of other turbine dynamics such as the tower. Nonetheless, these blade and tower interactions can be exploited to estimate the tower movement from the blade load sensors. As a consequence, the aim of this paper is to analyse the observability properties of the blade and tower model and based on these insights, an estimator design is proposed to reconstruct the tower motion from the measurements of the flap-wise blade loads, that are typically available to the IPC. The proposed estimation strategy offers many immediate benefits, for example, the estimator obviates the need for hardware sensor redundancy, and the estimated signals can be used for control or fault monitoring purposes. We further show results obtained from high-fidelity turbine simulations to demonstrate the performance of the proposed estimator.**

***Index Terms*—Estimator, Observer, Kalman filter, Individual blade-pitch control,**

I. Introduction

Large wind turbines often experience unsteady and intermittent aerodynamic loads from the wind and such loads inevitably cause fatigue damage to the turbine structures. To attenuate such harmful loads on blades and rotor structures, an increasing number of modern turbines employ individual pitch control (IPC) strategies alongside the collective pitch control (CPC). The role of the CPC is to regulate the rotor speed in above-rated conditions by collectively adjusting the pitch angle of each blade by the same amount [1]. The IPC provides additional pitch demand signals, in response to measurements of the flap-wise blade root bending moments [2]. As the size of a wind turbine increases, couplings between the turbine structures becomes more pronounced. Typically, and for reasons of simplicity of implementation favoured by the industry, IPCs are designed separately from a CPC and prudently to avoid excitation of other turbine structure dynamics [3]–[6]. Nonetheless, the interactions between the turbine blades and tower provide opportunities for an estimation problem in that the tower motions can be reconstructed based on the blade load measurements that are already available to the IPC.

However, systematic studies of the observability properties of the wind turbine structural systems have been somewhat neglected in the mainstream literature, albeit the use of estimation strategies have been reported in many applications in wind turbines. For example, wind speeds across the turbine rotor were estimated based on an aerodynamic turbine structural model [4], [7]. In addition, an observer was employed to estimate the unknown system states for state-feedback control strategies [8]. Moreover, previous work [9] proposed a method to estimate blade load based on sensors locating at the non-rotating turbine structure. Nevertheless, analysis of the observability of the structural turbine models provides useful insights of how much information of the unknown dynamics can be extracted from the available measurements. Thus, this work is motivated to investigate the observability properties of the tower estimation problem.

Typically, measurements of the flap-wise blade loads are obtained from sensing devices that are located at the blade root upon a rotating coordinate frame (e.g. [2]–[6]), whilst the turbine tower fore-aft movements are upon a stationary reference frame relative to the rotor. Thus, such periodically time-varying nature of the turbine structural system makes the observability study and estimator design non-trivial by the substantial and mature linear time-invariant control theories.

Therefore, this work aims to bridge the gap by demonstrating the observability analysis of the periodic blade and tower model. Subsequently, Coleman transformations are employed for transforming the periodic system into a time-invariant model and its observability is then studied. With these insights, this work finally proposes an estimator design that can reconstruct tower motions from the blade moment measurements. There are significant benefits from an industrial perspective: firstly, the virtual sensor obviates the need for more hardware redundancy; secondly, the estimated tower movement signals can be employed for supervisory and control purposes.

The remainder of this paper is structured as follows. Section II describes the preliminaries on the observability and periodic systems. Section III provides a background of the blade and tower modelling. In Section IV, analysis of observability of the modelled system and transformations of the periodic system are presented. Subsequently, an estimator for tower disturbance are designed in Section V. In Section VI, the performance of the estimator is demonstrated using high-fidelity wind turbine simulations. Finally, Section VII concludes the paper with a summary and an overview of future work.

Notation

Let $\mathbb{R}$, $\mathbb{C}$ and $\mathbb{Z}$ denote the real and complex fields and and set of integers, respectively, $j := \sqrt{1}$ and let $s \in \mathbb{C}$ denote a complex variable. The space $\mathcal{R}$ denotes the space of proper

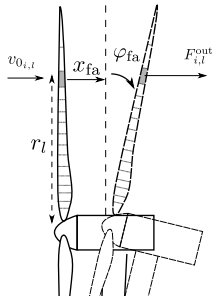

Fig. 1: An out-of-plane force $F^{\rm out}_{i,l}$ is caused by the stream-wise wind speed $v_{0_{i,l}}$ on the shaded blade element at r_l, fore-aft tower $\dot{x}_{\rm fa}$ and rotational velocity $\dot{\varphi}_{\rm fa}$.

real-rational transfer function matrices and $\dot{x}$ represents the time derivative of x. Let $v^T \in \mathbb{R}^{1\times n_v}$ denote the transpose of a vector $v \in \mathbb{R}^{n_v}$ and $V^T \in \mathbb{R}^{n_y\times n_z}$ is the transpose of a matrix $V \in \mathbb{R}^{n_z\times n_y}$. The identity matrix is denoted as I.

II. Preliminaries on observability and linear periodic systems

This section recalls a few definitions and theorems pertinent to linear time-periodic systems.

Definition 2.1: (Linear time-periodic system). A linear time-periodic system is described as follows:

$$\dot{x}(t) = A(t)x(t) + Bu(t),\ y(t) = Cx(t), \tag{1}$$

with state $x \in \mathbb{R}^{n_x}$, input $u \in \mathbb{R}^{n_u}$, output $y \in \mathbb{R}^{n_y}$ and $A(t) \in \mathbb{R}^{n_x\times n_x}$ is periodic with period T, namely $A(t) := A(t+T)$.

Definition 2.2: (State transition matrix). There exists a matrix $\Phi(t, t_0)$ of (1) mapping states $x(t_0)$ at t_0 to states $x(t)$ at t.

Theorem 2.1: [10]. The linear time-periodic system (1) is asymptotically stable if and only if the eigenvalues of the state transition $\Phi(T, 0)$ lie within the unit circle.

Definition 2.3: (Observability Gramian) The observability Gramian of (1) are:

$$W_o(t_0, t_{\rm f}) := \int_{t_0}^{t_{\rm f}} \Phi^T(t, t_0)C^T C\Phi(t, t_0)dt. \tag{2}$$

Theorem 2.2: [11] The system (1) is observable over the time interval $[t_0, t_{\rm f}]$ if and only if $W_o(t_0, t_{\rm f})$ is positive definite.

III. Modelling of blade and tower dynamics

This section gives a brief background of the blade and tower model including their interactions and shows such a model is asymptotically stable.

Typical aerodynamic interactions of a typical wind turbine are depicted in Figure 1, where the shapes of the blades along the span-wise locations are optimised accordingly for maximising the power output. Thus, the wind forces are not uniformly distributed on the blades and to model such forces, blade element momentum theory is often adopted [12], where the blade is divided to small length elements as shown in Figure 1. Consider three turbine blades are identical, the out-of-plane forces $F^{\rm out}_{i,l}$ for each blade $i \in \{1, 2, 3\}$ on the span-wise element $l \in \{1, \cdots, L\} \subset \mathbb{Z}$ is defined as follows:

$$F^{\rm out}_{i,l}(t) := \frac{dF^{\rm out}_{i,l}}{d\theta}\theta_i(t) + \frac{dF^{\rm out}_{i,l}}{dv}v_{i,l}(t), \tag{3}$$

where $\theta_i(t)$ denotes the pitch angle of blade i and $v_{i,l}$ is the stream-wise wind speed. The variations of out-of-plane forces with respect to the pitch angle and wind speed are represented as $\frac{dF^{\rm out}_{i,l}}{d\theta} \in \mathbb{R}$ and $\frac{dF^{\rm out}_{i,l}}{dv} \in \mathbb{R}$, where these values are obtained under an uniform wind condition of 18 $\rm ms^{-1}$, chosen because this value is near the centre of the range of wind speeds covering the above-rated wind conditions. Subsequently, Figure 1 revealed that the stream-wise wind speed $v_{i,l}$ experienced by the blades are subjected to the fore-aft velocity $\dot{x}_{\rm fa}$ and rotational velocity $\dot{\varphi}_{\rm fa}$ the tower-top, defined as follows:

$$v_{i,l}(t) := v_{0_{i,l}}(t) - \dot{x}_{\rm fa}(t) + \dot{\varphi}_{\rm fa}(t)r_l \sin\big(\phi_i(t)\big), \tag{4}$$

where the free stream-wise wind speed is $v_{0_{i,l}}$. The azimuth angle of each blade is denoted as $[\phi_1(t), \phi_2(t), \phi_3(t)] = [\phi(t), \phi(t) + \frac{2\pi}{3}, \phi(t)]$ and $\phi(t)$ is defined as the angle of the first blade from the horizontal yaw axis. This work implicitly assumes the tower is a prismatic beam so that the ratio between rotation and displacement is $\frac{2}{3h}$ where $h \in \mathbb{R}$ is the height of the tower (e.g. [4], [3]). Thus, the fore-aft rotational velocity of the tower-top can be approximated as $\dot{\varphi}_{\rm fa}(t) \approx \frac{2}{3h}\dot{x}_{\rm fa}(t)$.

Assuming the wind forces on the turbine hub are negligible, the aerodynamic thrust $F_{\rm a}$ on the tower-top and flap-wise blade moments $M_{{\rm a}_i}$ acting on the blades are defined as follows:

$$F_{\rm a}(t) := \sum_{i=1}^{3}\sum_{l=0}^{L} F^{\rm out}_{i,l}(t), \tag{5}$$

$$M_{{\rm a}_i}(t) := \sum_{l=0}^{L} F^{\rm out}_{i,l}(t)r_l \tag{6}$$

where r_l denotes the blade length between the blade root to the blade element l as shown in Figure 1. Substituting (3) into (5) yields:

$$F_{\rm a}(t) := \frac{dF_{\rm a}}{d\theta}\bar{\theta}(t) + F^{\rm d}_{\rm a}(t) - k_{Fx}\dot{x}_{\rm fa}(t), \tag{7a}$$

$$M_{{\rm a}_i}(t) := \frac{dM_{\rm a}}{d\theta}\theta_i(t) + M^{\rm d}_i(t) - k_{Mx}\dot{x}_{\rm fa}(t) + k_{M\varphi}\dot{x}_{\rm fa}(t)\sin\big(\phi_i(t)\big) \tag{7b}$$

where $\bar{\theta}(t) := \frac{1}{3}\big(\theta_1(t) + \theta_2(t) + \theta_3(t)\big)$ is the collective pitch angle and the remaining variables are described by:

$$\frac{dF_{\rm a}}{d\theta} := \sum_{i=1}^{3}\sum_{l=0}^{L}\frac{dF^{\rm out}_{i,l}}{d\theta}, F^{\rm d}_{\rm a}(t) := \sum_{i=1}^{3}\sum_{l=0}^{L}\frac{dF^{\rm out}_{i,l}}{dv}v_{0_{i,l}}(t), \tag{7c}$$

$$\frac{dM_{\rm a}}{d\theta} := \sum_{l=0}^{L}\frac{dF^{\rm out}_{i,l}}{d\theta}r_l,\ M^{\rm d}_i(t) := \sum_{l=0}^{L}\frac{dF^{\rm out}_{i,l}}{dv}r_l v_{0_{i,l}}(t) \tag{7d}$$

$$k_{Fx} := \sum_{i=1}^{3}\sum_{l=0}^{L}\frac{dF^{\rm out}_{i,l}}{dv},\ k_{Mx} := \sum_{l=0}^{L}\frac{dF^{\rm out}_{i,l}}{dv}r_l,\ k_{M\varphi} := \frac{2}{3h}k_{Mx}. \tag{7e}$$

Notice that the wind-induced thrust $F^{\rm d}_{\rm a}$ is typically the averaged force across the rotor, thus, it can be expressed in terms of the averaged wind-induced blade disturbance

$\bar{M}^{\mathrm{d}}(t) := \frac{1}{3}\big(M_1^{\mathrm{d}}(t)+M_2^{\mathrm{d}}(t)+M_3^{\mathrm{d}}(t)\big)$, as $F_{\mathrm{t}}^{\mathrm{d}}(t) = \bar{M}(t)r_{\mathrm{eff}}^{-1}$, where $r_{\mathrm{eff}} := \sum_{l=0}^{L} r_l \in \mathbb{R}$.

Consequently, the dynamics of the flap-wise blade root bending moments M_i for blade i and fore-aft motion of the tower-top $\dot{x}_{\mathrm{fa}}$ can be modelled as follows (e.g. [3], [4]):

$$\ddot{M}_i(t) + 2\zeta_{\mathrm{b}}\omega_{\mathrm{b}}\dot{M}_i(t) + \omega_{\mathrm{b}}^2 M_i(t) = \omega_{\mathrm{b}}^2 M_{\mathrm{a}_i}(t), \tag{8a}$$

$$\ddot{x}_{\mathrm{fa}}(t) + 2\zeta_{\mathrm{t}}\omega_{\mathrm{t}}\dot{x}_{\mathrm{fa}}(t) + \omega_{\mathrm{t}}^2 x_{\mathrm{fa}}(t) = \omega_{\mathrm{t}}^2\big(F_{\mathrm{a}}(t) + \frac{2}{3h}M_{\mathrm{tilt}}(t)\big), \tag{8b}$$

where $\zeta_{\mathrm{b}}, \zeta_{\mathrm{t}} \in \mathbb{R}$ denote the damping ratio of the blade and tower, whilst $\omega_{\mathrm{b}}, \omega_{\mathrm{t}} \in \mathbb{R}$ represent the natural frequency of the blade and tower. The tilt moment of rotor is defined as $M_{\mathrm{tilt}}(t) := \sum_{i=1}^{3} M_i(t)\sin(\phi_i(t))$.

The state-space representation of (8) can be formulated as follows:

$$\begin{aligned} \dot{x}(t) &= A(t)x(t) + Bu(t) + B_{\mathrm{d}}d(t), \\ y(t) &= Cx(t), \end{aligned} \tag{9a}$$

with

$$x(t) = \begin{bmatrix}\dot{\mathbf{M}}(t) & \mathbf{M}(t) & \dot{x}_{\mathrm{fa}}(t) & x_{\mathrm{fa}}(t)\end{bmatrix}^T \in \mathbb{R}^{n_x}, \tag{9b}$$

$$u(t) = \begin{bmatrix}\theta_1(t) & \theta_2(t) & \theta_3(t)\end{bmatrix}^T \in \mathbb{R}^{n_u}, \tag{9c}$$

$$d(t) = \begin{bmatrix}M_1^{\mathrm{d}} & M_2^{\mathrm{d}} & M_3^{\mathrm{d}}\end{bmatrix}^T \in \mathbb{R}^{n_d}, \tag{9d}$$

$$y(t) = \mathbf{M}(t) \in \mathbb{R}^{n_y}, \tag{9e}$$

$$A(t) = \begin{bmatrix} -2\zeta_{\mathrm{b}}\omega_{\mathrm{b}}I & -\omega_{\mathrm{b}}^2 I & -k_{Mx}\mathbf{1} + k_{M\varphi}\mathbf{S}(\phi) & 0 \\ I & 0 & 0 & 0 \\ 0 & \frac{2}{3h}\mathbf{S}(\phi)^T & -2\zeta_{\mathrm{t}}\omega_{\mathrm{t}} - k_{Fx}\omega_{\mathrm{t}}^2 & -\omega_{\mathrm{t}}^2 \\ 0 & 0 & 1 & 0 \end{bmatrix}, \tag{9f}$$

$$B = \begin{bmatrix} \omega_{\mathrm{b}}^2 \frac{dM_{\mathrm{a}}}{d\theta} I \\ 0 \\ \omega_{\mathrm{t}}^2 \frac{1}{3}\frac{dF_{\mathrm{a}}}{d\theta}\mathbf{1}^T \\ 0 \end{bmatrix},\ B_{\mathrm{d}} = \begin{bmatrix} \omega_{\mathrm{b}}^2 I \\ 0 \\ \omega_{\mathrm{t}}^2 \frac{1}{3} r_{\mathrm{eff}}^{-1}\mathbf{1}^T \\ 0 \end{bmatrix}, \tag{9g}$$

$$C = \begin{bmatrix}0 & I & 0 & 0\end{bmatrix}, \tag{9h}$$

where $\mathbf{M}(t) := [M_1(t), M_2(t), M_3(t)]^T$, $\mathbf{S}(\phi) := [\sin(\phi(t)), \sin(\phi(t)+\frac{2\pi}{3}), \sin(\phi(t)+\frac{4\pi}{3})]^T$, $\mathbf{1} := [1,1,1]^T$ and $I \in \mathbb{R}^{3\times 3}$ is an identity matrix. Notice that $\phi(t) := \omega(t)t$, where $\omega(t)$ is the rotor speed.

Remark 1: An implicit assumption in the linear system (9) is that the rotor operates at a rated speed $\omega(t) = \omega_0$ in the above-rated wind conditions, as that implies $\phi(t) := \omega_0 t$. Thus, the system (9) is a linear periodic system with the period of $T = \frac{2\pi}{\omega_0}$.

Lemma 3.1: Under an assumption of a fixed rotor speed $\omega(t) = \omega_0$, the linear periodic system (9) is asymptotically stable.

Proof: Given that the system (9) is a linear periodic system, from Theorem 2.1, direct numerical integration of (9) [13] showed that the eigenvalues of $\Phi(T,0)$ of (9) are all within the unit circle. Thus, the system (9) is asymptotically stable. ∎

IV. Analysis of the system observability

This section examines the observability properties of the linear system (9). Subsequently, transformations are introduced which transform the linear time-varying system into a time-invariant system, for which a substantial body of mature estimation theory can immediately brought to bear upon the design of tower disturbance estimator.

A. Observability of the periodic system

Lemma 4.1: Assume a constant rotor speed $\omega(t) = \omega_0$, the linear periodic system (9) is observable over the interval $[t_0, t_{\mathrm{f}}]$.

Proof: Given that system (9) is asymptotically stable as proved in Lemma 3.1, to examine the observability of (9), from Theorem 2.2, the observability Gramian $W_o(t_0, t_{\mathrm{f}})$ of (9):

$$W_0(t_0, t_{\mathrm{f}}) = \int_{t_0}^{t_{\mathrm{f}}} \Phi^T(t, t_0)C^T C^T \Phi(t, t_0)dt, \tag{10}$$

needs to be positive definite. However, finding the analytical expression of $\Phi(t, t_0)$ and $W_0(t_0, t_{\mathrm{f}})$ is not trivial for time-varying systems like (9). Nonetheless, there is a theorem proposed by [14] that can examine the observability without computing the state transition. Assume $A(t) \in \mathbb{R}^{n_x \times n_x}$ and $C \in \mathbb{R}^{n_y \times n_x}$ are $q-1$ and q times continuously differentiable, respectively, and consider a matrix defined as follows:

$$N(t) = [N_0(t), \cdots, N_q(t)]^T, \tag{11a}$$

where

$$N_0(t) = C, \tag{11b}$$

$$N_{m+1} = N_m A(t) + \dot{N}_m,\ m = 1, 2, \cdots, q, \tag{11c}$$

If $N(t)$, where $t \in [t_0, t_{\mathrm{f}}]$, has rank n_x, then $W_0(t_0, t_{\mathrm{f}})$ is positive definite [14]. Consider $q = 3$, $N(t)$ becomes:

$$N(t) = \begin{bmatrix} 0 & I & 0 & 0 \\ I & 0 & 0 & 0 \\ -2\omega_{\mathrm{b}}\zeta_{\mathrm{b}}I & -\omega_{\mathrm{b}}^2 I & N^{(3,3)}(t) & 0 \\ (4\omega_{\mathrm{b}}^2\zeta_{\mathrm{b}}^2 - \omega_{\mathrm{b}}^2)I & N^{(4,2)}(t) & N^{(4,3)}(t) & N^{(4,4)}(t) \end{bmatrix}, \tag{12a}$$

where

$$N^{(3,3)}(t) = k_{M\varphi}(S)(\omega_0 t) - k_{Mx}\mathbf{1}, \tag{12b}$$

$$N^{(4,2)}(t) = 2\zeta_{\mathrm{b}}\omega_{\mathrm{b}}^3 I - \frac{3}{2h}\mathbf{S}(\phi(t))\big(k_{Mx}\mathbf{1} - k_{M\varphi}\mathbf{S}^T(\phi(t))\big), \tag{12c}$$

$$N^{(4,3)}(t) = \big(k_{Fx}\omega_{\mathrm{t}}^2 + 2\zeta_{\mathrm{t}}\omega_{\mathrm{t}} + 2\zeta_{\mathrm{b}}\omega_{\mathrm{b}}\big)\times \big(k_{Mx}\mathbf{1} - k_{M\varphi}\mathbf{S}(\phi(t))\big) + k_{M\varphi}\dot{\mathbf{S}}(\phi(t)), \tag{12d}$$

$$N^{(4,4)}(t) = \omega_{\mathrm{t}}^2(k_{Mx}\mathbf{1} - k_{M\varphi}\mathbf{S}(\phi(t))(\omega_0 t)). \tag{12e}$$

It is clear that $N(t)$ has rank n_x over $t \in [t_0, t_{\mathrm{f}}]$. Thus, the system (9) is observable. ∎

Lemma 4.1 indicates that use of observers can reconstruct the tower disturbance based on the periodic model (9). However, it is non-trivial to design an observer based on periodic models, the periodic model (9) can be transformed into a time-invariant model, as discussed in the following section.

B. Transformations of the periodic systems

The measurements of the flap-wise blade root bending moments are obtained upon a rotating frame of reference, whilst the tower fore-aft motion is on a fixed co-ordinate frame. Thus, the Coleman transformations [15] can be employed to accommodate the mixed reference frame nature.

The typical Coleman transform $T_{\rm cm}(\phi(t)) \in \mathbb{R}^{3\times 3}$ is defined as follows [15]:

$$\begin{bmatrix} \bar{M}(t) \\ M_{\rm tilt}(t) \\ M_{\rm yaw}(t) \end{bmatrix} := \underbrace{\frac{2}{3}\begin{bmatrix} 1 & 1 & 1 \\ \sin(\phi(t)) & \sin\left(\phi(t)+\frac{2\pi}{3}\right) & \sin\left(\phi(t)+\frac{4\pi}{3}\right) \\ \cos(\phi(t)) & \cos\left(\phi(t)+\frac{2\pi}{3}\right) & \cos\left(\phi(t)+\frac{4\pi}{3}\right) \end{bmatrix}}_{T_{\rm cm}(\phi(t))} \times \begin{bmatrix} M_1(t) \\ M_2(t) \\ M_3(t) \end{bmatrix}. \tag{13a}$$

where $M_{\rm tilt}, M_{\rm yaw}$ denote the collective tilt and yaw referred flap-wise blade root bending moments, respectively. The inverse Coleman transform $T^{\rm inv}_{\rm cm}(\phi(t)) \in \mathbb{R}^{3\times 3}$ is as follows:

$$\begin{bmatrix} M_{\rm a_1}(t) \\ M_{\rm a_2}(t) \\ M_{\rm a_3}(t) \end{bmatrix} := \underbrace{\begin{bmatrix} 1 & \sin(\phi(t)) & \cos(\phi(t)) \\ 1 & \sin\left(\phi(t)+\frac{2\pi}{3}\right) & \cos\left(\phi(t)+\frac{2\pi}{3}\right) \\ 1 & \sin\left(\phi(t)+\frac{4\pi}{3}\right) & \cos\left(\phi(t)+\frac{4\pi}{3}\right) \end{bmatrix}}_{T^{\rm inv}_{\rm cm}(\phi(t))} \begin{bmatrix} \bar{M}_{\rm a}(t) \\ M_{\rm a_{tilt}}(t) \\ M_{\rm a_{yaw}}(t) \end{bmatrix} \tag{13b}$$

where $\bar{M}_{\rm a}, M_{\rm a_{tilt}}, M_{\rm a_{yaw}}$ represent the collective, tilt and yaw referred aerodynamic forces upon a non-rotating reference frame, respectively.

Lemma 4.2: Under a given fixed rotor speed ω_0 and Coleman transformations (13), the linear periodic (9) can be transformed into the following time-invariant form:

$$\begin{bmatrix} \dot{\xi}(t) \\ \dot{x}_{\rm t}(t) \end{bmatrix} = \underbrace{\begin{bmatrix} A_\xi & B_{\xi{\rm t}} \\ B_{\rm tM} & A_{\rm t} \end{bmatrix}}_{A_{\rm z}} \underbrace{\begin{bmatrix} \xi(t) \\ x_{\rm t}(t) \end{bmatrix}}_{z(t)} + \underbrace{\begin{bmatrix} B_{\xi\theta} \\ B_{{\rm t}\theta} \end{bmatrix}}_{B_{\rm z}} u_{\rm cm}(t) + \underbrace{\begin{bmatrix} B_{\xi{\rm d}} \\ B_{\rm td} \end{bmatrix}}_{B_{\rm d_z}} d_{\rm cm}(t),$$
$$y_{\rm cm}(t) = \underbrace{\begin{bmatrix} C_\xi & 0 \end{bmatrix}}_{C_{\rm z}} z(t) \tag{14a}$$

with $z \in \mathbb{R}^{n_z}$ the referred measurements of flap-wise blade moments, pitch angle signals and wind-induced blade disturbance upon a non-rotating coordinate frame are defined as follows:

$$y_{\rm cm}(t) = \left[\bar{M}(t), M_{\rm tilt}(t), M_{\rm yaw}(t)\right]^T \in \mathbb{R}^{n_y} \tag{14b}$$
$$u_{\rm cm}(t) = \left[\bar{\theta}(t), \theta_{\rm tilt}(t), \theta_{\rm yaw}(t)\right]^T \in \mathbb{R}^{n_u} \tag{14c}$$
$$d_{\rm cm}(t) = \left[\bar{M}^{\rm d}(t), M^{\rm d}_{\rm tilt}(t),\ M^{\rm d}_{\rm yaw}(t)\right]^T \in \mathbb{R}^{n_d} \tag{14d}$$

where $A_{\rm z} \in \mathbb{R}^{n_z\times n_z}$ is Hurwitz. The matrices $A_{\rm z}, B_{\rm z}, B_{\rm d_z}, C_{\rm z}$ are obtained from (19), (20), (21) and (22).

Proof: The proof uses the following properties:

$$\begin{aligned} \mathcal{L}[u(t)\sin\phi(t)] &= \mathcal{L}\Big[u(t)\frac{j(e^{-j\omega_0 t} - e^{j\omega_0 t})}{2}\Big], \\ &= \frac{j}{2}(u(s+j\omega_0) - u(s-j\omega_0)), \end{aligned} \tag{15a}$$

$$\begin{aligned} \mathcal{L}\left[u(t)\cos\phi(t)\right] &= \mathcal{L}\left[u(t)\frac{e^{j\omega_0 t} + e^{-j\omega_0 t}}{2}\right] \\ &= \frac{1}{2}\left(u(s-j\omega_0) + u(s+j\omega_0)\right) \end{aligned} \tag{15b}$$

where $u(t)$ is an arbitrary input signal, $u(s)$ is its Laplace transform and $\phi(t) = \omega_0 t$ is assumed. Substituting identities (15a) into Coleman transformations (13) yields:

$$\begin{bmatrix} \bar{M}(s) \\ M_{\rm tilt}(s) \\ M_{\rm yaw}(s) \end{bmatrix} := \frac{2}{3}C_- \begin{bmatrix} M_1(s-j\omega_0) \\ M_2(s-j\omega_0) \\ M_3(s-j\omega_0) \end{bmatrix} + \frac{2}{3}C_+ \begin{bmatrix} M_1(s+j\omega_0) \\ M_2(s+j\omega_0) \\ M_3(s+j\omega_0) \end{bmatrix}, \tag{16a}$$

$$\begin{bmatrix} M_{\rm a_1}(s) \\ M_{\rm a_2}(s) \\ M_{\rm a_3}(s) \end{bmatrix} := C_-^T \begin{bmatrix} \bar{M}_{\rm a}(s) \\ M_{\rm a_{tilt}}(s-j\omega_0) \\ M_{\rm a_{yaw}}(s-j\omega_0) \end{bmatrix} + C_+^T \begin{bmatrix} \bar{M}_{\rm a}(s) \\ M_{\rm a_{tilt}}(s+j\omega_0) \\ M_{\rm a_{yaw}}(s+j\omega_0) \end{bmatrix}, \tag{16b}$$

where C_- and C_+ are defined as:

$$C_- := \frac{1}{2}\begin{bmatrix} 2 & 0 & 0 \\ 0 & 1 & -j \\ 0 & j & 1 \end{bmatrix} \begin{bmatrix} \frac{1}{2} & \frac{1}{2} & \frac{1}{2} \\ \sin(0) & \sin(\frac{2\pi}{3}) & \sin(\frac{4\pi}{3}) \\ \cos(0) & \cos(\frac{2\pi}{3}) & \cos(\frac{4\pi}{3}) \end{bmatrix}, \tag{16c}$$

$$C_+ := \frac{1}{2}\begin{bmatrix} 2 & 0 & 0 \\ 0 & 1 & j \\ 0 & -j & 1 \end{bmatrix} \begin{bmatrix} \frac{1}{2} & \frac{1}{2} & \frac{1}{2} \\ \sin(0) & \sin(\frac{2\pi}{3}) & \sin(\frac{4\pi}{3}) \\ \cos(0) & \cos(\frac{2\pi}{3}) & \cos(\frac{4\pi}{3}) \end{bmatrix}. \tag{16d}$$

Consider the blade model upon a rotating frame of reference (8a) and its Laplace transform:

$$M_i(s) = G(s)M_{\rm a_i}(s), \tag{17}$$

where $G(s) := C_{\rm b}(sI - A_{\rm b})^{-1}B_{\rm b}$, with $A_{\rm b} \in \mathbb{R}^{n_{\rm b}\times n_{\rm b}}, B_{\rm b} \in \mathbb{R}^{n_{\rm b}}, C_{\rm b} \in \mathbb{R}^{1\times n_{\rm b}}$. Subsequently, substituting the model (17) into (16) yields the following Coleman-transformed model upon a fixed co-ordinate frame:

$$\begin{bmatrix} \bar{M}(s) \\ M_{\rm tilt}(s) \\ M_{\rm yaw}(s) \end{bmatrix} := \begin{bmatrix} G(s) & 0 & 0 \\ 0 & G_+(s) & G_-(s) \\ 0 & -G_-(s) & G_+(s) \end{bmatrix} \begin{bmatrix} \bar{M}_{\rm a}(s) \\ M_{\rm a_{tilt}}(s) \\ M_{\rm a_{yaw}}(s) \end{bmatrix} \tag{18a}$$

where $G_+, G_- \in \mathcal{R}$ are real and proper transfer functions defined as follows:

$$G_+(s) := \frac{G(s+j\omega_0) + G(s-j\omega_0)}{2}, \tag{18b}$$

$$G_-(s) := j\frac{G(s+j\omega_0) - G(s-j\omega_0)}{2} \tag{18c}$$

and $G(s+j\omega_0) := C_{\rm b}(sI - (A_{\rm b} - j\omega_0 I))^{-1}B_{\rm b}$ and $G(s - j\omega_0) := C_{\rm b}(sI - (A_{\rm b} + j\omega_0 I))^{-1}B_{\rm b}$. Subsequently, the Coleman transformed model (18) can be expressed in a state-space form, with state $x_{\rm cm} \in \mathbb{C}^{5n_{\rm b}}$, as follows:

$$\dot{x}_{\rm cm}(t) = A_{\rm cm}x_{\rm cm}(t) + B_{\rm cm}M_{\rm a_{cm}}(t),\ y_{\rm cm}(t) = C_{\rm cm}x_{\rm cm}(t), \tag{19a}$$

where $A_{\rm cm} \in \mathbb{C}^{5n_{\rm b}\times 5n_{\rm b}}$, $B_{\rm cm} \in \mathbb{C}^{5n_{\rm b}\times 3}$, $C_{\rm cm} \in \mathbb{R}^{3\times 5n_{\rm b}}$ are defined as follows:

$$A_{\rm cm} = \begin{bmatrix} A_{\rm b} & 0 & 0 & 0 & 0 \\ 0 & A_{\rm b} - j\omega_0 I & 0 & 0 & 0 \\ 0 & 0 & A_{\rm b} + j\omega_0 I & 0 & 0 \\ 0 & 0 & 0 & A_{\rm b} - j\omega_0 I & 0 \\ 0 & 0 & 0 & 0 & A_{\rm b} + j\omega_0 I \end{bmatrix}, \tag{19b}$$

$$B_{\rm cm} = \begin{bmatrix} B_{\rm b} & 0 & 0 \\ 0 & B_{\rm b} & jB_{\rm b} \\ 0 & B_{\rm b} & -jB_{\rm b} \\ 0 & -jB_{\rm b} & B_{\rm b} \\ 0 & jB_{\rm b} & B_{\rm b} \end{bmatrix}, C^T_{\rm cm} = \begin{bmatrix} C_{\rm b} & 0 & 0 \\ 0 & \frac{1}{2}C_{\rm b} & 0 \\ 0 & \frac{1}{2}C_{\rm b} & 0 \\ 0 & 0 & \frac{1}{2}C_{\rm b} \\ 0 & 0 & \frac{1}{2}C_{\rm b} \end{bmatrix}, \tag{19c}$$

and $M_{a_{\rm cm}}$ can be obtained by substituting Coleman transform (13) into (7b):

$$M_{a_{\rm cm}}(t) = \frac{dM_{\rm a}}{d\theta}u_{\rm cm}(t) + d_{\rm cm}(t) + k_{Mx_{\rm cm}}\dot{x}_{\rm fa}(t), \tag{19d}$$

where $k_{Mx_{\rm cm}} = \left[-k_{Mx}, k_{M\varphi}, k_{M\varphi}\right]^T$. Equivalently, let a similarity transformation matrix $T \in \mathbb{C}^{5n_{\rm b}\times 5n_{\rm b}}$, such that $x_{\rm cm} \in \mathbb{C}^{5n_{\rm b}}$ is mapped into $\xi = Tx_{\rm cm} \in \mathbb{R}^{5n_{\rm b}}$, define as follows:

$$T := \begin{bmatrix} 1 & 0 & 0 \\ 0 & T_{\rm c} & 0 \\ 0 & 0 & T_{\rm c} \end{bmatrix},\ T_{\rm c} = \frac{1}{2}\begin{bmatrix} (1+j) & (1-j) \\ (1-j) & (1+j) \end{bmatrix} \tag{20}$$

The equivalent model of (19) with the real-valued state ξ becomes:

$$\dot{\xi}(t) = A_\xi \xi(t) + B_\xi M_{\mathrm{a_{cm}}}(t),\ y_{\mathrm{cm}}(t) = C_\xi \xi(t), \tag{21a}$$

where

$$A_\xi = T A_{\mathrm{cm}} T^{-1} = \begin{bmatrix} A_{\mathrm{b}} & 0 & 0 & 0 & \\ 0 & A_{\mathrm{b}} & -\omega_0 I & 0 & 0 \\ 0 & \omega_0 I & A_{\mathrm{b}} & 0 & 0 \\ 0 & 0 & 0 & A_{\mathrm{b}} & -\omega_0 I \\ 0 & 0 & 0 & \omega_0 I & A_{\mathrm{b}} \end{bmatrix}, \tag{21b}$$

$$B_\xi = T B_{\mathrm{cm}} = \begin{bmatrix} B_{\mathrm{b}} & 0 & 0 \\ 0 & B_{\mathrm{b}} & B_{\mathrm{b}} \\ 0 & B_{\mathrm{b}} & -B_{\mathrm{b}} \\ 0 & -B_{\mathrm{b}} & B_{\mathrm{b}} \\ 0 & B_{\mathrm{b}} & B_{\mathrm{b}} \end{bmatrix},\ C_\xi = C_{\mathrm{cm}} T^{-1} = C_{\mathrm{cm}}. \tag{21c}$$

Let the tower dynamics model (8b) in state-space form be:

$$\begin{bmatrix} \ddot{x}_{\mathrm{fa}}(t) \\ \dot{x}_{\mathrm{fa}}(t) \end{bmatrix} = \underbrace{\begin{bmatrix} -2\omega_{\mathrm{t}}\zeta_{\mathrm{t}} & -\omega_{\mathrm{t}}^2 \\ 1 & 0 \end{bmatrix}}_{A_{\mathrm{t}}} \underbrace{\begin{bmatrix} \dot{x}_{\mathrm{fa}}(t) \\ x_{\mathrm{fa}}(t) \end{bmatrix}}_{x_{\mathrm{t}}(t)} + \underbrace{\begin{bmatrix} \frac{dF_{\mathrm{a}}}{d\theta} E_1 \\ 0 \end{bmatrix}}_{B_{\mathrm{t}\theta}} u_{\mathrm{cm}}(t) + \underbrace{\begin{bmatrix} \frac{dM_{\mathrm{a}}}{dv} r_{\mathrm{eff}}^{-1} E_1 \\ 0 \end{bmatrix}}_{B_{\mathrm{td}}} d_{\mathrm{cm}}(t) + \underbrace{\begin{bmatrix} \frac{3}{2h} C_\xi^{(2,:)} \\ 0 \end{bmatrix}}_{B_{\mathrm{t}\xi}} \xi(t). \tag{22}$$

where $E_1 = [\omega_{\mathrm{t}}^2, 0, 0]$ and $C_\xi^{(2,:)}$ denotes the second row of C_ξ. Finally, augmenting (21) with the tower dynamics (22) yields (14). ∎

Lemma 4.3: The linear time-invariant system (14) is observable.

Proof: Given that the model (14) is linear time-invariant, the observability proof can be established if the observability matrix has full rank. The observability matrix $\mathcal{O}$ of (14) is defined as follows:

$$\mathcal{O} := \begin{bmatrix} C_{\mathrm{z}} & C_{\mathrm{z}} A_{\mathrm{z}} & \cdots & C_{\mathrm{z}} A_{\mathrm{z}}^{n_z - 1} \end{bmatrix}^T, \tag{23}$$

which has rank n_z. Thus, the system (14) is observable. ∎

Results from Lemma 4.2 and 4.3 indicate the time-invariant form of the linear blade and tower model (9) is observable, that lay the foundation for observer design in the following section.

V. Estimation and control for tower vibrations

This section presents an estimator design. Figure 2 depicts the architecture of the proposed system, where the estimator reconstructs the fore-aft velocity of the tower-top $\hat{\dot{x}}_{\mathrm{fa}}$ based on the blade moment measurements $\bar{M}, \tilde{M}_{\mathrm{tilt}}, \tilde{M}_{\mathrm{yaw}}$ and pitch signals $\bar{\theta}, \tilde{\theta}_{\mathrm{tilt}}, \tilde{\theta}_{\mathrm{yaw}}$ upon a fixed co-ordinate frame.

The estimator employed in this work is an unknown input disturbance observer [16] that uses the modelled system (14) augmented with a wind-induced disturbance model. For brevity, a constant wind-induced disturbance model is assumed (e.g. [4]):

$$\dot{d}_{\mathrm{cm}}(t) = 0, \tag{24}$$

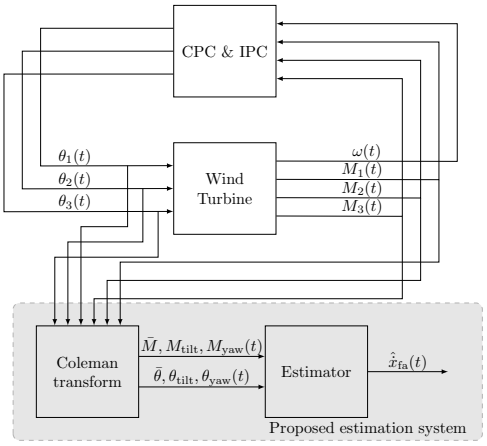

Fig. 2: Schematic of the proposed estimator.

Thus, the augmented model is described as follows:

$$\begin{bmatrix} \dot{\hat{z}}(t) \\ \dot{\hat{d}}_{\mathrm{cm}}(t) \end{bmatrix} = \begin{bmatrix} A_{\mathrm{z}} & B_{\mathrm{d_z}} \\ 0 & 0 \end{bmatrix} \begin{bmatrix} \hat{z}(t) \\ \hat{d}_{\mathrm{cm}}(t) \end{bmatrix} + \begin{bmatrix} B_{\mathrm{z}} \\ 0 \end{bmatrix} u_{\mathrm{cm}}(t) + L(y_{\mathrm{cm}}(t) - \begin{bmatrix} C_{\mathrm{z}} & 0 \end{bmatrix} \begin{bmatrix} \hat{z}(t) \\ \hat{d}_{\mathrm{cm}}(t) \end{bmatrix}), \tag{25}$$

where the hat symbol denotes estimate and L represents estimator gain, which can be optimised by Kalman filtering theory [17].

Theorem 5.1: The augmented system (25) is detectable.

Proof: The proof is based on that the pair $\{A_{\mathrm{z}}, C_{\mathrm{z}}\}$ is observable and the following conditions [18] :

$$\mathrm{rank} \begin{bmatrix} I - A_{\mathrm{z}} & B_{\mathrm{b_z}} \\ C_{\mathrm{z}} & 0 \end{bmatrix} = n_z + n_d \tag{26}$$

∎

Remark 2: Results from Theorem 5.1 is equivalently to say that the fore-aft motion of the tower-top can be reconstructed based on the referred blade moments upon a fixed coordinate.

VI. Numerical results and discussion

This section presents simulation results to demonstrate the performance of the proposed estimator and estimation-based controller for the tower fore-aft motion. The turbine model employed in this work is the NREL 5MW turbine [19] and the simulations are carried out on FAST [20]. The high-fidelity turbine model is of much greater complexity than the model (25) employed in the estimator and with the exception of the yaw axis, all degrees-of-freedom were enabled, including flap-wise and edge-wise blade modes, in addition to the tower and shaft dynamics. Simulations in this study were conducted under a turbulent wind field with a mean wind speed 18 ms^{-1} and turbulence intensity of 16%, generated from TurbSim [21], chosen since this value is near the centre of the range of wind speeds covering above-rated wind conditions.

A. Performance of estimator

The performance was compared by examining the estimated signals of the tower fore-aft velocity and the actual measurements from the simulation turbine. Figure 3(a) illustrates

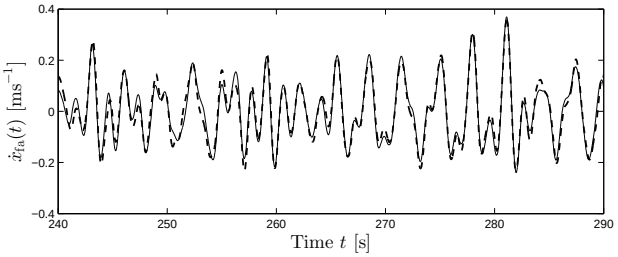

(a) Estimate $\hat{\dot{x}}_{\rm fa}(t)$ (dash line) and actual measurement $\dot{x}_{\rm fa}(t)$ (solid line) of the tower-top velocity signal.

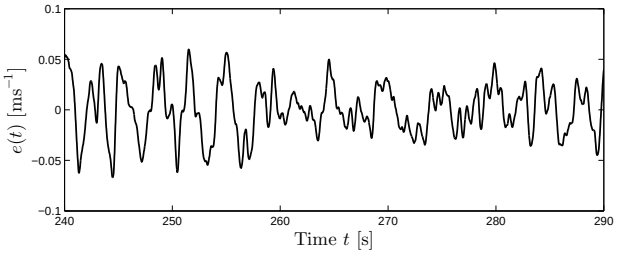

(b) The error between the estimate and actual signals of tower-top fore-aft velocity.

Fig. 3: Time histories of wind speed at the hub height, estimate and actual measurement of tower-top velocity and error.

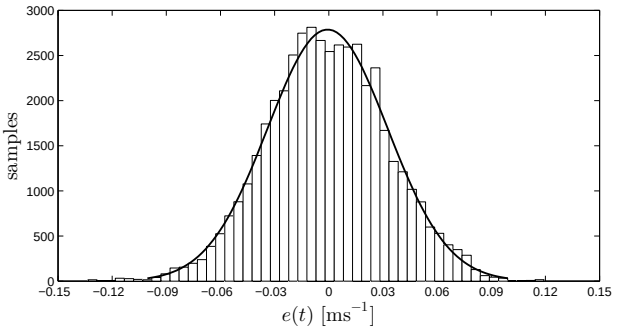

Fig. 4: Histogram of the error between the estimate and actual signals of tower-top fore-aft velocity. Bar represents the error samples and solid line shows a Gaussian distribution.

the time histories of the estimates alongside actual signals of the tower-top fore-aft velocity. It can be seen that the estimate matches the actual signal well across the above-rated wind conditions. Nonetheless, there exist slight differences in magnitude as shown in Figure 3(a). Such small discrepancies arise from the model uncertainties in the blade model and disturbance models. Nevertheless, Figure 3(b) reveals the time series of the error between these two signals $e(t)$ where the maximum error is no larger than $\pm 0.06 \mathrm{ms}^{-1}$. Interestingly, by running the simulation long enough, the error has a Gaussian distribution with mean value of $0 \mathrm{ms}^{-1}$ and standard deviation of $0.033 \mathrm{ms}^{-1}$, as evident by the histogram in Figure 4.

VII. Conclusion

This paper has presented analysis on observability of the periodic blade and tower system and the Coleman transformed time-invariant system. Based on these insights, this current work subsequently proposed an estimator for reconstructing the tower-top motion based on measurements of the blade that are already accessible to the IPC. Analytical and numerical results are presented that show the estimator based on a Coleman-transformed blade model can perform good and reliable estimations. Future work will look to extend the concepts of tower disturbance estimation to an offshore floating wind turbine.

References

[1] LY Pao and KE Johnson. A tutorial on the dynamics and control of wind turbines and wind farms. *Proc. of ACC*, 2009.

[2] E. A. Bossanyi. Individual Blade Pitch Control for Load Reduction. *Wind Energy*, 6(2):119–128, 2003.

[3] T G van Engelen. Design model and load reduction assessment for multi-rotational mode individual pitch control (higher harmonics control). In *Proc. of European Wind Energy Conference*, number March, pages 6–68, 2006.

[4] K. Selvam, S. Kanev, J. W. van Wingerden, T. van Engelen, and M. Verhaegen. Feedback-feedforward individual pitch control for wind turbine load reduction. *International Journal of Robust and Nonlinear Control*, 19(1):72–91, 2009.

[5] Qian. Lu, R. Bowyer, and B.Ll. Jones. Analysis and design of Coleman transform-based individual pitch controllers for wind-turbine load reduction. *Wind Energy*, 18(8):1451–1468, 2015.

[6] Wai Hou Lio, Bryn Ll. Jones, Qian Lu, and J.A. Rossiter. Fundamental performance similarities between individual pitch control strategies for wind turbines. *International Journal of Control*, pages 1–16, 2015.

[7] K Z Østergaard, P Brath, and J Stoustrup. Estimation of effective wind speed. *Journal of Physics: Conference Series*, 75:012082, 2007.

[8] E. a. Bossanyi. The Design of closed loop controllers for wind turbines. *Wind Energy*, 3(3):149–163, 2000.

[9] M. Jelavic, V. Petrovic, and N. Peric. Individual pitch control of wind turbine based on loads estimation. In *Annual Conference of IEEE Industrial Electronics*, 2008.

[10] Roger W. Brockett. *Finite Dimensional Linear Systems*. New York Wiley, 1970.

[11] Henry D'Angelo. *Linear time-varying systems: analysis and synthesis*. Allyn and Bacon, 1970.

[12] Tony Burton, Nick Jenkins, David Sharpe, and Ervin Bossanyi. *Wind Energy Handbook*. John Wiley & Sons, Ltd, Chichester, UK, 2011.

[13] Pierre Montagnier, Raymond J Spiteri, and Jorge Angeles. The control of linear time-periodic systems using FloquetLyapunov theory. *International Journal of Control*, 2004.

[14] Chi Tsong Chen. *Linear System Theory and Design*. Oxford University Press, 1984.

[15] Robert P. Coleman and Arnold M. Feingold. Theory Of Self-Excited Mechanical Oscillations Of Helicopter Rotors With Hinged Blades. *National Advisory Committee for Aeronautics,*, page Report 1351, 1958.

[16] C. D. Johnson. Accommodation of External Disturbances in Linear Regulator and Servomechanism Problems. *IEEE Transactions on Automatic Control*, 16(6):635–644, 1971.

[17] R. E. Kalman. A New Approach to Linear Filtering and Prediction Problems. *Journal of Basic Engineering*, 82(1):35, 1960.

[18] Gabriele Pannocchia and James B. Rawlings. Disturbance models for offset-free model predictive control. *AIChE Journal*, 49(2):426–437, 2003.

[19] J. Jonkman, S. Butterfield, W. Musial, and G. Scott. Definition of a 5-MW Reference Wind Turbine for Offshore System Development. Technical report, National Renewable Energy Laboratory (NREL), Golden, CO, 2009.

[20] J.M. Jonkman and M.L. Buhl Jr. FAST User's Guide. Technical report, National Renewable Energy Laboratory (NREL), 2005.

[21] B.J. Jonkman. TurbSim User's Guide. Technical report, National Renewable Energy Laboratory (NREL), 2009.